



المؤتمر السادس للعلوم الهندسية والتقنية  
The Sixth Conference for Engineering Sciences and Technology (CEST-6)  
Conference Proceeding homepage: <https://cest.org.ly>



## Optimizing Extended Kalman Filter for Speed Sensorless Control of Induction Motors Using Artificial Bee Colony Algorithm

\*Abobkr Hamid, Mohamed Darfoun

Electrical Engineering Department, College of Engineering Technology, Houn, Libya.

### Keywords:

ABC algorithm  
EKF  
Estimation speed  
Induction motors

### ABSTRACT

Implementing sensor less control in induction motor drives has significantly reduced expenses and hardware weight while enhancing reliability. Among the highly effective speed sensor less control techniques, the Extended Kalman Filter (EKF) is distinguished by its superior estimation accuracy. However, the efficiency of the EKF relies on the accurate determination of noise covariance matrices. Recently, many studies have aimed to optimize these matrices to enhance performance. In this research, we introduce a unique method for speed estimation in an induction motor drive using the Artificial Bee Colony (ABC) algorithm to maximize the performance of EKF. The effectiveness of the proposed method is validated by the Matlab/Simulink simulation of a constant Voltage/Hertz controller-based drive system at different operating conditions.

تحسين مرشح كالمان الممتد للتحكم في سرعة المحركات الحثية بدون مستشعر السرعة باستخدام خوارزمية مستعمرة النحل الاصطناعية

\*أبوبكر حامد و محمد دارفون

قسم الهندسة الكهربائية، كلية التقنية الهندسية، هون، ليبيا.

### الكلمات المفتاحية:

خوارزمية ABC  
EKF  
تقدير السرعة  
المحركات الحثية

### الملخص

لقد أدى تطبيق نظم التحكم الغير معتمدة على مستشعرات السرعة في المحرك الحثي إلى تقليل التكاليف والوزن الإجمالي للأجهزة بشكل كبير، مع تعزيز الموثوقية في نفس الوقت. يعتبر مرشح كالمان الممتد (EKF) من تقنيات التحكم بدون استخدام مستشعرات السرعة الأكثر فعالية حيث يتميز هذا المرشح بدقة تقدير فائقة. ومع ذلك، فإن كفاءة هذا المرشح تعتمد على التحديد الدقيق لمصفوفات التباين الضوضائي. مؤخراً، هدفت العديد من الدراسات إلى تحسين هذه المصفوفات لتعزيز أداء المرشح في عملية تقدير السرعة. في هذا البحث، نقدم طريقة فريدة لتقدير السرعة في نظام محرك حثي باستخدام خوارزمية مستعمرة النحل الاصطناعية (ABC) لتحسين أداء مرشح كالمان الممتد. تم التحقق من فعالية الطريقة المقترحة من خلال المحاكاة باستخدام برنامج Matlab/Simulink لنظام يعتمد على التحكم بثابت الجهد/التردد (Voltage/Hertz) في ظل ظروف تشغيلية مختلفة.

### 1. Introduction

In modern induction motor (IM) control applications, speed measurement is critical to controlling rotor speed accurately. Rotor speed is typically determined by installing sensors or using calibration cables on the motor's rotating shaft. However, these measurements mounted on the shaft may reduce the drive system's reliability and robustness. Additionally, they can increase system costs and motor weight due to the extra space required for mounting [1]. As a result, sensor less control methods have been implemented to solve these problems.

There has been a notable surge in interest recently in developing sensor less methods for IM. These methods are utilized to estimate the rotor speed. In addition, important information for the control system is provided through state variables of the IM, including rotor flux

\*Corresponding author:

E-mail addresses: [a.abobkr@ceh.edu.ly](mailto:a.abobkr@ceh.edu.ly), (M. Darfoun) [m.darfoun@ceh.edu.ly](mailto:m.darfoun@ceh.edu.ly)

linkage, rotor current components, and electromagnetic torque, which are difficult to measure directly [2]. The sensor less methods have been categorized into two main classifications: the signal injection-based method and the model-based IM state equations method [3], [4].

The signal injection-based method is commonly employed in sensor less control applications for permanent magnet synchronous motors (PMSM). This method performs extremely well at low speeds and even at zero speed. Nevertheless, its performance becomes limited as the speed increases [5], [6]. Model-based methods are commonly used in sensor less IM applications for estimating speed and IM parameters, which primarily involve Sliding-Mode Observers [7], Artificial Neural Networks [8], and the Extended Kalman Filter [1], [2], [9], [10], [11], [12], [13], [14], [15], [16], [17]. These methods rely on the

mathematical model of the IM, with their estimation processes essentially depending on the back electromotive force (EMF) [6].

R.E. Kalman introduced the Kalman filter (KF), a linear recursive algorithm for stochastic dynamic systems, in 1960 [18]. R.E. Kalman and R.S. Bucy first introduced the EKF, a modified version of the KF, in 1961 [19]. Compared to other nonlinear model-based sensor less control methods, the EKF is a promising model-based method and one of the best estimating methods for a stochastic system, especially when the noise model and the system are undefined, such as in the IM [2] [9]. Consequently, over the past two decades, the EKF has emerged as the most widely used estimator for sensor less IM control applications [10]. In sensor less control applications of induction motors (IM) utilizing the EKF, the EKF offers superior noise filtering for both the system and measurements, provided the noise covariances are known. The system noise covariance is denoted by  $Q$ , while  $R$  represents the measurement noise covariance [11].

While the EKF has been successfully applied to speed sensor less control of IM, several challenges remain. One significant issue is accurately determining the filter noise covariance matrices to improve EKF performance. As a result, the noise matrices are treated as adjustable parameters that require careful fine-tuning [10]. These values are classically determined through a method of trial and error, which takes a lot of time and tedious, and often fails to produce precise speed estimations [11], [12], [13], [14], [15].

Recently, several intelligent optimization algorithms have been developed to reduce the time and effort needed to find the best values for noise covariance matrices. These algorithms aim to find more efficient approaches for defining noise covariance matrices, leading to significant improvements in the process.

The covariance matrix of measurement noise ( $R$ ), and the covariance matrix of system noise ( $Q$ ), and the statistical measure have all been optimized using the Genetic Algorithm (GA). weight matrix ( $G$ ) for the EKF, aiming to estimate speed in closed-loop constant V/f control and field-oriented control of IM[11]. Recently, other evolutionary algorithms have been utilized for this purpose. For instance, Particle Swarm Optimization (PSO) has been used in closed-loop sensor less Direct Torque Control (DTC) [9], and a modified PSO was introduced in [16]. PSO has also been used without feedback control [10]. Additionally, the Enhanced Fireworks Algorithm (EFA) has been investigated to improve the EKF's noise covariance matrices [12].

The ABC algorithm is a method that simulates an artificial bee colony has been effectively used to solve challenging issues [20], [21]. This approach is based on an evolutionary algorithm that was motivated by honey bees' hunt for the optimal food source [22]. In [17], the ABC-based EKF for IM speed estimation is shown. But as far as the authors are aware, no one has used the ABC algorithm for EKF speed estimate in sensor less control systems of IM.

In this paper, we integrated the ABC algorithm into a speed sensor less drive system to improve the optimization of noise covariance matrices. The EKF performs better with this new method, especially when it comes to speed estimation for sensor-less control of IM by optimizing the execution of the EKF. The ABC algorithm is chosen for its efficiency in finding the optimal parameters that minimize estimation errors, leading to more accurate and reliable speed estimation under various operational conditions. By optimizing the noise covariance matrices, the EKF's sensitivity to model inaccuracies and external disturbances is significantly reduced, thereby improving the robustness and precision of the control system. This approach specifically addresses the challenges associated with the sensor less control of IM, ensuring that the EKF can maintain high performance even in the absence of direct speed measurements. The application of the ABC algorithm in this context is essential for achieving these improvements, and it highlights the potential of bio-inspired optimization techniques in enhancing traditional control methods.

Simulation studies were conducted on a constant V/f controlled IM drive with closed-loop control. The simulation results confirm that the ABC-optimized EKF effectively and accurately estimates speed for sensor less IM applications.

The paper is structured into seven sections. The next section introduces the state model of the IM. Section III introduces the EKF algorithm. Sections IV and V discuss the ABC optimization method and its application in optimizing the EKF, respectively. Section VI

covers simulations, Section VII discusses the results and performance analyses, and the conclusion is presented in Section VIII.

## 2. State Model of Induction Motor

It is an input-voltage continuous dynamic model used in the simulated system for IM. In this fifth-order IM model, the state variables of the model, represented by the d and q components in the are represented by the stator reference frame, and the mechanical variables are the rotor speed and stator currents and rotor fluxes. It is well known that in filtering applications, the measurements are available only at integral multiples of the sample time period ( $T$ ). Consequently, the EKF is a discrete-time system, whereas the IM is a continuous-time system. To apply the EKF to the IM, the continuous-time system must be discretized using the Forward Euler method as follows [24]:

$$x_{n+1} = A_n x_n + B_n u_n + G_n w_n \quad (1)$$

$$y_n = C_n x_n + v_n \quad (2)$$

Where:

$$x_n = \begin{bmatrix} i_{ds}^{(n)} \\ i_{qs}^{(n)} \\ \lambda_{dr}^{(n)} \\ \lambda_{qr}^{(n)} \\ \omega_r^{(n)} \end{bmatrix} \quad u_n = \begin{bmatrix} V_{ds}^{(n)} \\ V_{qs}^{(n)} \end{bmatrix} \quad y_n = \begin{bmatrix} i_{ds}^{(n)} \\ i_{qs}^{(n)} \end{bmatrix}$$

$$A_n = \begin{bmatrix} 1 - \frac{K_r}{K_l} T & 0 & \frac{L_M R_r}{L_r^2 K_l} T & \frac{P L_M \omega_r^{(n)}}{2 L_r K_l} T & 0 \\ 0 & 1 - \frac{K_r}{K_l} T & \frac{P L_M \omega_r^{(n)}}{2 L_r K_l} T & \frac{L_M R_r}{L_r^2 K_l} T & 0 \\ \frac{L_M}{\tau_r} T & 0 & 1 - \frac{1}{\tau_r} T & -\frac{P}{2} \omega_r^{(n)} T & 0 \\ 0 & \frac{L_M}{\tau_r} T & \frac{P}{2} \omega_r^{(n)} T & 1 - \frac{1}{\tau_r} T & 0 \\ 0 & 0 & 0 & 0 & 1 \end{bmatrix}$$

$$B_n = \begin{bmatrix} \frac{T}{K_l} & 0 \\ 0 & \frac{T}{K_l} \\ 0 & 0 \\ 0 & 0 \\ 0 & 1 \end{bmatrix} \quad c_n = \begin{bmatrix} 1 & 0 & 0 & 0 & 0 \\ 0 & 1 & 0 & 0 & 0 \end{bmatrix}$$

Here are the variables and parameters used:

- $x_n$  : represents the state variables of the IM ;
- $u_n$  : represents the inputs of the IM at time n;
- $y_n$  : represents the measured values of the IM;
- $i_{ds}, i_{qs}$  : stator current components;
- $\lambda_{ds}, \lambda_{qs}$  : rotor flux components;
- $V_{ds}, V_{qs}$  : stator voltage components;
- $\omega_r$  : the rotor speed;
- $T$  : the sampling time;
- $R_s, R_r$  : stator and rotor resistance respectively;
- $L_s, L_r$  : stator and rotor inductance respectively;
- $L_m$  : mutual inductance;
- $P$  : number of poles;

The following terms are derived from the above parameters:

$$K_r = R_s + L_M^2 R_r / L_r^2$$

$$K_l = (1 - L_M^2 / L_r / L_s) \times L_s$$

$$\tau_r = L_r / R_r$$

Further,  $G$  is the noise-weight matrix in, and  $w$  represents the noise matrix of the system, that is IM noise. The noise matrix of the observed output of the model reads, or measurement noise, is represented by  $v$  in equation (2) [11]. It is assumed that  $w$  and  $v$  have zero-mean Gaussian distributions [12]. These noises' covariance matrices have the following definition [11]:

$$Q = cov(w) \quad (3)$$

$$R = cov(v) \quad (4)$$

Where:

$Q$ : covariance matrix of the induction motor noise.

$R$ : covariance matrix of the measurement noise.

## 3. EKF Algorithm for Speed Estimation

The EKF algorithm employs recursive equations to compute predicted values based on IM inputs, which serve as one of the two EKF inputs. These predicted values are then compared with the measured values obtained from IM outputs, representing the second EKF input. The estimated state-space vector of the IM is computed using the error resulting from the previous comparison. This error is multiplied by a gain called the Kalman filter gain (K) to reduce it. This gain is calculated using the matrices G, Q, and R. Therefore, to accurately estimate the rotor speed, which is an element of the state vector in the IM, the values of these matrices must be chosen carefully.

Since (1) represents the dynamic model of the IM and because the matrix ( $A_n$ ) consists of the rotor speed, the IM becomes a nonlinear dynamic system [12]. The state transition function ( $\Phi$ ) represents the dynamics of the system (IM), describing how the state variables change over T as follows [12]:

We can denote  $x_{n+1} = \Phi$

Where:

$$\Phi = \begin{pmatrix} \left(1 - \frac{K_r}{K_l} T\right) i_{ds}^{(n)} + \frac{L_M R_r}{L_r^2 K_l} T \lambda_{dr}^{(n)} + \frac{P L_M \omega_r^{(n)}}{2 L_r K_l} T \lambda_{qr}^{(n)} + \frac{T}{K_l} V_{ds}^{(n)} \\ \left(1 - \frac{K_r}{K_l} T\right) i_{qs}^{(n)} - \frac{P L_M \omega_r^{(n)}}{2 L_r K_l} T \lambda_{dr}^{(n)} + \frac{L_M R_r}{L_r^2 K_l} T \lambda_{qr}^{(n)} + \frac{T}{K_l} V_{qs}^{(n)} \\ \frac{L_M}{\tau_r} T i_{ds}^{(n)} + \left(1 - \frac{1}{\tau_r} T\right) \lambda_{dr}^{(n)} - \frac{P}{2} \omega_r^{(n)} T \lambda_{qr}^{(n)} \\ \frac{L_M}{\tau_r} T i_{qs}^{(n)} + \frac{P}{2} \omega_r^{(n)} T \lambda_{dr}^{(n)} + \left(1 - \frac{1}{\tau_r} T\right) \lambda_{qr}^{(n)} \\ \omega_r^{(n)} \end{pmatrix} \quad (5)$$

Since the EKF is processing measurements in discrete time, the EKF will linearize the nonlinear state transition function,  $\Phi$  around the current estimate for every time step. One can do this through the Jacobian matrix [12].

$$\frac{\partial \Phi}{\partial x} = \begin{pmatrix} 1 - \frac{K_r}{K_l} T & 0 & \frac{L_M R_r}{L_r^2 K_l} T & \frac{P L_M \omega_r^{(n)}}{2 L_r K_l} T & \frac{L_M R_l}{L_r K_l} \\ 0 & 1 - \frac{K_r}{K_l} T & -\frac{P L_M \omega_r^{(n)}}{2 L_r K_l} T & \frac{L_M R_r}{L_r^2 K_l} T & -\frac{P L_l}{2 L_r} \\ \frac{L_M}{\tau_r} T & 0 & 1 - \frac{1}{\tau_r} T & -\frac{P}{2} \omega_r^{(n)} T & -T \\ 0 & \frac{L_M}{\tau_r} T & \frac{P}{2} \omega_r^{(n)} T & 1 - \frac{1}{\tau_r} T & T \\ 0 & 0 & 0 & 0 & 0 \end{pmatrix} \quad (6)$$

The EKF process consists of two repeated steps [17]. The first step is the prediction, the estimated state matrix for the next time step ( $\hat{x}_{n+1}$ ) is calculated using the estimated state matrix for the current time step ( $\hat{x}_n$ ). This process can be represented mathematically as follows:

$$\hat{x}_{n+1} = f(\hat{x}_n, u_n) \quad (7)$$

Initially,  $\hat{x}_n$  is assumed to be a zero ( $5 \times 1$ ) matrix. Additionally, another prediction must be made for the error covariance matrix for the next time step ( $\hat{P}_{n+1}$ ), as described in (8).

$$\hat{P}_{n+1} = \frac{\partial \Phi}{\partial x} \Big|_{x=x_n} P_n \frac{\partial \Phi^T}{\partial x} \Big|_{x=x_n} + G Q G^T \quad (8)$$

Here,  $P_n$  is the estimated error covariance matrix for the current time, initially assumed to be a  $5 \times 5$  unit matrix. Moreover,  $P_{n+1}$  is used with the measurement noise to compute the Kalman gain ( $K_n$ ).

$$K_n = P_{n+1} c_n^T (c_n P_{n+1} c_n^T + R)^{-1} \quad (9)$$

Here,  $c_n$  is the measurement matrix, which specifies the state variables corresponding to the measured values. In this paper, the measured values are  $i_{ds}$  and  $i_{qs}$ . Therefore,  $c_n$  should be defined as follows:

$$c_n x_n = \begin{bmatrix} 1 & 0 & 0 & 0 & 0 \\ 0 & 1 & 0 & 0 & 0 \end{bmatrix} \times \begin{bmatrix} i_{ds}^{(n)} \\ i_{qs}^{(n)} \\ \lambda_{dr}^{(n)} \\ \lambda_{qr}^{(n)} \\ \omega_r^{(n)} \end{bmatrix} = \begin{bmatrix} i_{ds}^{(n)} \\ i_{qs}^{(n)} \end{bmatrix} \quad (10)$$

The second step is the estimation, and once the Kalman gain is calculated, the updated state estimate ( $\hat{x}_n$ ) can be calculated using the following expression:

$$\hat{x}_n = \hat{x}_{n+1} + K_n [y_n - c_n \hat{x}_{n+1}] \quad (11)$$

From (11), It is worth noting here that the contribution of the Kalman gain is to mitigate the error obtained by comparing the true measured values  $y_n$  with the estimated measured values  $c_n \hat{x}_{n+1}$ . Moreover, the updated error covariance matrix  $P_n$  is calculated through using the relation below:

$$P_n = P_{n+1} - K_n c_n P_{n+1} \quad (12)$$

#### 4. ABC Optimization

The ABC technique is an optimization technique that draws inspiration from honeybee foraging behavior. Developed to mimic the way bees explore fields and search for the richest flowers, this algorithm is employed to solve by striking a balance between search space exploitation and exploration in complex optimization problems [22]. Three different bee species make up a honeybee swarm: worker bees, observer bees, and scout bees [25].

1. **Employed bees:** They conduct random searches for food sources (solutions) and communicate their findings, which include nectar amounts, to other bees in the hive through dancing. The duration of the dance reflects the nectar amount (fitness value) of the food source.
2. **Onlooker bees:** They watch the dances of different working bees and choose good food sources according to their quality.
3. **Scout bees:** When an employed bee from an abandoned food supply randomly searches for a new food source, a scout bee is created.

The Bees Algorithm relies on several key mathematical equations to execute its steps:

*Step 1. Initialization*

An initial population  $x_{ij}$  is generated randomly across the D-dimensional problem space using (13):

$$x_{ij} = x_j^{\min} + \text{rand}[0,1] \times (x_j^{\max} - x_j^{\min}) \quad (13)$$

Where,  $i = \{1, 2, \dots, SN\}$  represents the number of food sources,  $j = \{1, 2, \dots, D\}$  denotes the number of optimization parameters,  $x_j^{\min}$  and  $x_j^{\max}$  are lower and upper boundary parameters for the solution respectively,  $\text{rand}[0,1]$  generates uniformly distributed random values between 0 and 1.

*Step2. Employed Bees*

Each bee sequentially visits a food source and explores the vicinity of the reference position to find an optimal new position  $v_{ij}$ . Equation (14) is utilized for this search:

$$v_{ij} = x_{ij} + \varphi_{ij} \times (x_{ij} - x_{kj}) \quad (14)$$

Where,  $k = \{1, 2, \dots, SN\}$  and  $j = \{1, 2, \dots, D\}$  are randomly chosen indices, and  $k \neq j$ ,  $\varphi_{ij}$  is a random number in the range  $[-1, 1]$ ,  $x_{ij}$  represents the position of the reference food source and  $x_{kj}$  is a randomly selected food source in the same dimension. After updating, the new solution  $v_{ij}$  is compared with the reference  $x_{ij}$ . If the solution is as good as or better than the reference, it replaces the reference; otherwise, the reference is retained in a process known as greedy selection.

*Step 3. Onlooker Bees*

Observer bees use information from working bees to select food sources. They choose a food source based on a quality-related likelihood. Like working bees, every observer looks around its present location to come up with a fresh idea. After evaluating the new role, the

avaricious selection procedure is used. The probability that a food source  $x_{ij}$  is selected is determined by the expression:

$$x_{ij} = \frac{fit_i}{\sum_{k=1}^{SN} fit_k} \quad (15)$$

Where  $fit_i$  represents the fitness value of solution  $i$ , which is proportional to the nectar amount.  $SN$  is the number of food sources (equal to the number of employed bees). For minimization problems,  $fit_i$  can be calculated using the expression:

$$fit_i = \begin{cases} \frac{1}{1 + F_i} & \text{if } F_i > 0 \\ 1 + F_i & \text{if } F_i < 0 \end{cases} \quad (16)$$

Where  $F_i$  is the goal function's value.

#### Step 4. Scout Bees

If onlookers and employed bees fail to enhance a food source's position within a specified number of cycles (Limit), that food source is deemed abandoned. The employed bees associated with it transition to scout bees, tasked with randomly exploring for new food sources using (13). This iterative process continues for the maximum number of rounds, in which the optimal solution was discovered in each iteration is retained. By the end of this process, the result ensures the discovery of the global solution.

#### 5. Optimization of EKF using ABC

The EKF algorithm will be implemented in this article for a closed-loop Voltage/Hz controller; see Fig. 1. While the rotor speed is controlled by the PID speed control, the voltages that will be applied to the stator windings of the IM will be defined by the closed-loop Voltage/Hz controller, represented as ( $u_n$ ) to match the intended reference speed instruction ( $\omega^*$ ). The measured values, denoted as ( $y_n$ ), correspond to the stator currents, as per (2) and (10). The EKF takes in currents and voltages from the stator as inputs. Using these inputs, the EKF calculates the IM's state, which includes the rotor speed ( $\omega_{est}$ ), and uses that information as feedback to adjust the speed controller. Consequently, the speed sensors can be eliminated, resulting in a sensor less control system.

In this study, The dynamic performance of the Voltage/Hz control is enhanced by optimizing the parameters  $G$ ,  $Q$ , and  $R$  using the ABC algorithm. The ABC-EKF formula requires multiple iterations to reach the optimal solution. Consequently, the ABC-EKF algorithm is initially executed offline. Once the optimal values of  $G$ ,  $Q$ , and  $R$  are determined, they are then applied online to the closed-loop IM. The ABC-EKF algorithm can be described as follows:

- 1. Initialize the population:** The 5 diagonal elements of  $G$ , the 5 diagonal elements of  $Q$ , and the 2 elements of  $R$  are arranged into 12 dimensions. The ABC algorithm begins by randomly generating initial values for these 12 elements using (13).
- 2. For each iteration:**
  - Using the initial values of the covariance matrices, the rotor speed ( $\omega_{est}$ ), which represents the fifth element of the state ( $x_n$ ), is estimated by the EKF according to (11).
  - The fitness function, calculated as the mean square error (MSE) and shown in equation (17), is determined by the difference between ( $\omega_{est}$ ) and ( $\omega_{meas}$ ). The MSE is utilized to evaluate the effectiveness of the various solutions obtained.

$$MSE = \frac{\sum_{i=1}^n (\omega_{meas} - \omega_{est})^2}{n} \quad (17)$$

- Based on the lowest MSE, the ABC calculates the optimal 12 elements of the covariance matrices using (14), (15), and (16).
- The optimal 12 elements are then applied to update the EKF, leading to an update of the estimated speed using (8), (9), and (11).

This procedure continues until a specific number of iterations has been achieved; in this study, the number is 100. The optimized closed-loop constant Voltage/Hz control system with EKF is then operated using the values of  $G$ ,  $Q$ , and  $R$ . in real-time to estimate the rotor speed.

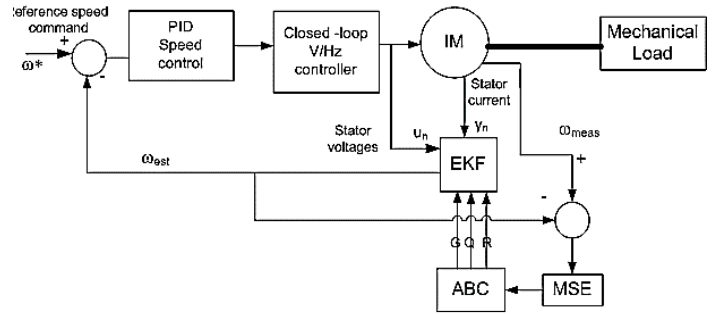


Fig. 1: Block diagram of a closed-loop constant Voltage/Hz control system with ABC-EKF for speed estimation

#### 6. Simulation

The system shown below serves as an example of the suggested technique for maximizing the covariance matrices. in Fig. 1 has been modeled in MATLAB/Simulink. Within the system illustrated in Fig. 1, the IM is represented by a Simulink block, while the EKF is implemented as a MATLAB s-function block. Furthermore, the ABC and MSE are scripted in m-files. The MSE plays a crucial role by acting as the interface between the ABC and EKF codes [17]. Fig. 2 presents the closed-loop Voltage/Hz control system with EKF speed estimate for the IM is implemented using Simulink.

The application of the real-coded ABC to optimize the EKF was performed by taking advantage of Simulink/MATLAB environment. Measured stator currents and stator voltages of the IM are two inputs to EKF. A three-phase squirrel cage IM is used in this study whose parameters are given in Table 1. In the optimization of ABC-EKF, source position of food is set to 20. Population size is equal to 240, while the number of bees is 20, the number of iterations is 100, the dimensional problem size is 12, and the lower and upper range is between 0.0001 and 0.1.

As an initial step, the ABC-EKF algorithm needs to be executed offline multiple times to converge to the optimal values of the noise matrices. This process was conducted using closed-loop V/f control of the IM drive, where the estimated speed is utilized as feedback for the input of the V/f controller.

With a simulation time of 1.5 seconds, the EKF can finish a number of different speed situations, including transient and steady states, as well as acceleration and deceleration. The sampling time ( $T$ ) has been set to  $1 \times 10^{-5}$  seconds. After 100 iterations of the ABC-EKF optimization, the optimal diagonal elements, determined by minimizing the mean squared error (MSE), are found to be:

$$G = \begin{bmatrix} 0.0001 & 0 & 0 & 0 & 0 \\ 0 & 0.0487 & 0 & 0 & 0 \\ 0 & 0 & 0.0001 & 0 & 0 \\ 0 & 0 & 0 & 0.0001 & 0 \\ 0 & 0 & 0 & 0 & 0.0636 \end{bmatrix}$$

$$Q = \begin{bmatrix} 0.0414 & 0 & 0 & 0 & 0 \\ 0 & 0.004 & 0 & 0 & 0 \\ 0 & 0 & 0.0001 & 0 & 0 \\ 0 & 0 & 0 & 0.0380 & 0 \\ 0 & 0 & 0 & 0 & 0.0755 \end{bmatrix}$$

$$R = \begin{bmatrix} 0.0171 & 0 \\ 0 & 0.0154 \end{bmatrix}$$

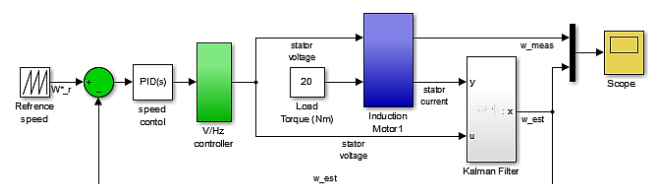


Fig. 2: Simulink model of closed-loop Voltage/Hz control with ABC-EKF for speed estimation

Table 1: Induction Motor Parameters [23]

7.5 Kw	220 V	6 poles	1160 rpm	60 Hz	Coefficient of friction Cf = 0.124
Rs = 0.282 Ω/phase	Rr = 0.151 Ω/phase	Ls = 0.0424 H/phase	Lr = 0.0417 H/phase	Lm = 0.0410 H/phase	Moment of inertia Jm = 0.4 kgm <sup>2</sup>

After optimizing the noise matrices, the next step is to apply these matrices online in the V/f closed-loop controller of the IM drive system.

**7. Results and Discussion**

To evaluate the efficacy of the ABC-EKF method for the constant V/f controller, different operational modes and the impact of changes in machine parameters were tested. Varied speed operations were achieved through the utilization of various commands that control the reference speed. خطأ! لم يتم العثور على مصدر المرجع. خطأ! لم يتم العثور على مصدر المرجع. display the estimated rotor speed (dotted line) obtained using the solid line is the optimized EKF with the actual rotor speed. The graphs show the relationship between the estimated and actual speeds during the acceleration mode, whether to 100 rad/sec or -100 rad/sec.

خطأ! لم يتم العثور على مصدر المرجع. depicts the ABC-EKF's performance in both transient and steady-state scenarios, demonstrating precise speed tracking in these situations.

Furthermore, a speed reversal command test was conducted from 120 rad/sec to -120 rad/sec, and a standstill condition was applied as shown in خطأ! لم يتم العثور على مصدر المرجع. خطأ! لم يتم العثور على مصدر المرجع. respectively. The results demonstrate that accurate speed tracking has been achieved.

Three tests with various stator and rotor resistance levels were carried out to look into how device parameters affected performance as a result of temperature rise and frequency shift of ABC-EKF for constant Voltage/Hertz controller, as Fig. 8 to 10 show. An analysis of the results of the tests indicates that:

- Among them, it is very sure that even under the worst conditions, when stator resistance increases by half and rotor resistance is doubled, the precision of speed tracking is still high.
- The EKF demonstrates the ability to reject disturbances caused by variations in machine parameters, as these variations are treated as noise in the algorithm used for speed estimation [9], [11].

All things considered, the ABC optimization approach for the EKF-based speed estimate method demonstrates excellent performance across various operating conditions and adapts to changes in machine parameters. However, the reliance on offline methods may lead to under severe circumstances, the ABC-EKF sensor-less control system's performance deteriorates [6], which is a recognized limitation of the proposed approach. Future work will focus on developing an online method for determining the noise covariance matrix.

Additionally, the iterative nature of the ABC algorithm may increase the computational burden. To mitigate this, a Reduced-order EKF (ROEKF) can be employed to reduce the computational demands while maintaining estimation accuracy, making it more suitable for real-time implementation in industrial applications with limited computational resources.

Additionally, the model and its discretized form may have limited applicability in specific IM conditions, such as high-speed operations and field-weakening modes. In these situations, the increased nonlinearity may reduce the accuracy of the linear approximations used in the EKF, leading to potential suboptimal performance in speed estimation. Future research should focus on incorporating advanced nonlinear estimation techniques, such as the Unscented Kalman Filter

(UKF), to improve performance and accuracy in these challenging operating conditions.

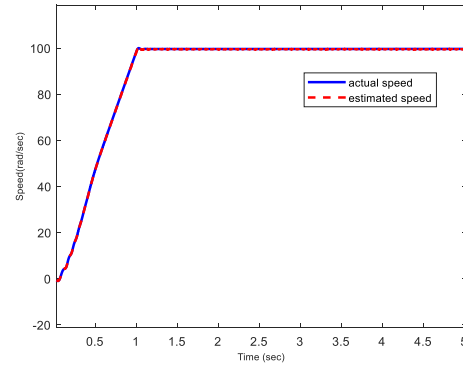


Fig. 3: Assessment of the ABC-EKF performance for a constant Voltage/Hertz drive while accelerating to 100 rad/sec

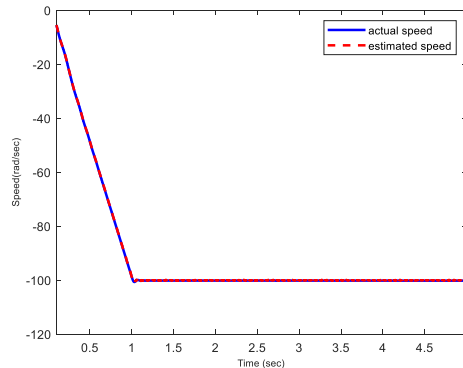


Fig. 4: Assessment of the ABC-EKF performance for a constant Voltage/Hertz drive while accelerating to -100 rad/sec.

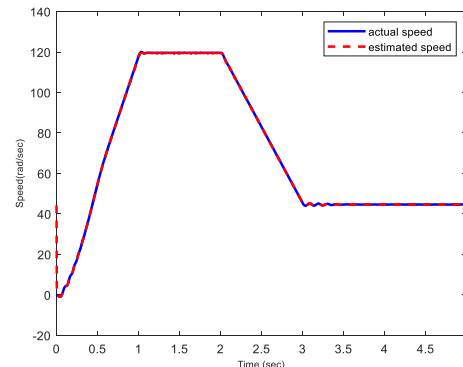


Fig. 5: Assessment of the ABC-EKF performance for a constant Voltage/Hertz drive during transient and steady-state conditions.

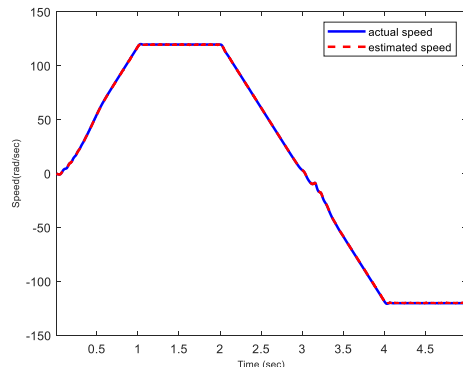


Fig. 6: Assessment of the ABC-EKF performance for a constant Voltage/Hertz drive during speed reversal from 120 to -120 rad/sec

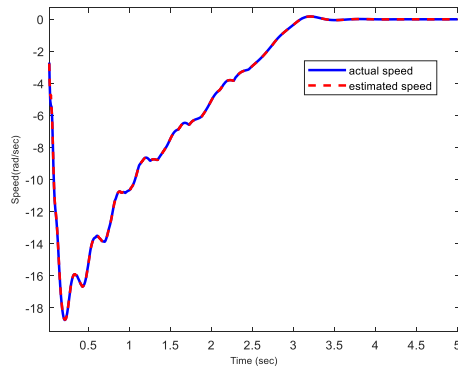


Fig. 7: Assessment of the ABC-EKF performance for a constant Voltage/Hertz drive during deceleration to a standstill

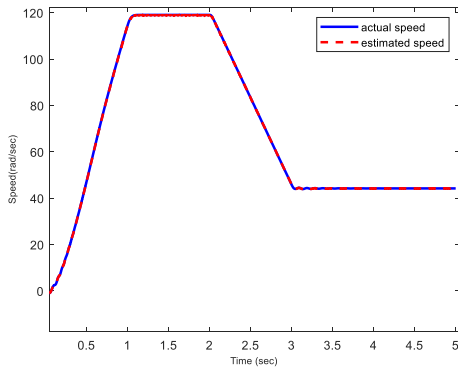


Fig. 8: Assessment of the ABC-EKF performance for a constant Voltage/Hertz drive when the  $R_s$  is increased by 50% and the  $R_r$  is increased by 100%

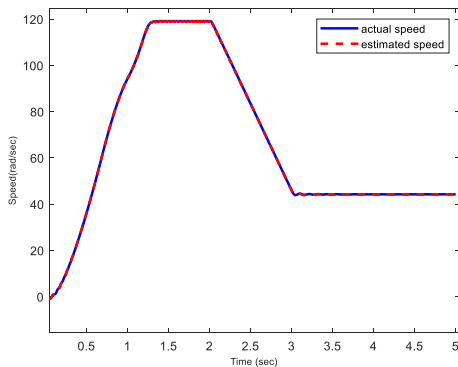


Fig. 9: Assessment of the ABC-EKF performance for a constant Voltage/Hertz drive when both the  $R_s$  and  $R_r$  are increased by 100%

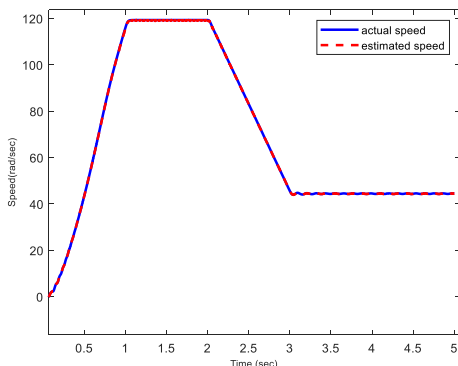


Fig. 10: Assessment of the ABC-EKF performance for a constant Voltage/Hertz drive when the  $R_s$  and  $R_r$  are both increased by 50%

## 8. Conclusion

This work presents a novel approach to improve the effectiveness of an EKF in determining an induction motor drive's speed. The weight and noise covariance matrices are optimally selected using the

artificial bee colony method. Studies using a constant Voltage/Hertz regulated induction motor drive in simulation confirm the efficacy of the suggested approach. The results show that precise speed tracking can be achieved at various speeds and during standstill conditions. Moreover, the method maintains high accuracy in speed tracking even under different disturbances, such as variations in stator and rotor resistance. This approach can replace the traditional trial-and-error method. Furthermore, it has established a framework for practical implementation of digital signal processing (DSP) /microcontroller hardware, which can be utilized in future sensor less induction motor drive systems.

## 9. References

- [1] O. Aydogmus and S. Sünter, "Implementation of EKF based sensorless drive system using vector controlled PMSM fed by a matrix converter," *International Journal of Electrical Power & Energy Systems*, vol. 43, no. 1, pp. 736–743, 2012, doi: <https://doi.org/10.1016/j.ijepes.2012.06.062>.
- [2] S. Chavez Velazquez, R. A. Palomares, and A. N. Segura, "Speed estimation for an induction motor using the extended Kalman filter," in *14th International Conference on Electronics, Communications and Computers, 2004. CONIELECOMP 2004.*, 2004, pp. 63–68. doi: 10.1109/ICECC.2004.1269550.
- [3] D. Xu, B. Wang, G. Zhang, G. Wang, and Y. Yu, "A review of sensorless control methods for AC motor drives," *CES Transactions on Electrical Machines and Systems*, vol. 2, no. 1, pp. 104–115, 2018, doi: 10.23919/TEMS.2018.8326456.
- [4] J. Holtz, "Sensorless Control of Induction Machines—With or Without Signal Injection?," *IEEE Transactions on Industrial Electronics*, vol. 53, no. 1, pp. 7–30, 2006, doi: 10.1109/TIE.2005.862324.
- [5] R. Ni, D. Xu, F. Blaabjerg, K. Lu, G. Wang, and G. Zhang, "Square-Wave Voltage Injection Algorithm for PMSM Position Sensorless Control With High Robustness to Voltage Errors," *IEEE Trans Power Electron*, vol. 32, no. 7, pp. 5425–5437, 2017, doi: 10.1109/TPEL.2016.2606138.
- [6] Z. Yin, F. Gao, Y. Zhang, C. Du, G. Li, and X. Sun, "A Review of Nonlinear Kalman Filter Applying to Sensorless Control for AC Motor Drives," *China Electrotechnical Society Transactions on Electrical Machines and Systems*, vol. 3, pp. 351–362, May 2019, doi: 10.30941/CESTEMS.2019.00047.
- [7] L. Wogi, M. Morawiec, and T. Ayana, "Sensorless Control of Induction Motor Based on Super-Twisting Sliding Mode Observer With Speed Convergence Improvement," *IEEE Access*, vol. 12, pp. 74239–74250, 2024, doi: 10.1109/ACCESS.2024.3404040.
- [8] X. Sun, L. Chen, Z. Yang, and H. Zhu, "Speed-Sensorless Vector Control of a Bearingless Induction Motor With Artificial Neural Network Inverse Speed Observer," *IEEE/ASME Transactions on Mechatronics*, vol. 18, no. 4, pp. 1357–1366, 2013, doi: 10.1109/TMECH.2012.2202123.
- [9] I. M. Alsofyani, N. R. N. Idris, T. Sutikno, and Y. A. Alamri, "An optimized Extended Kalman Filter for speed sensorless direct torque control of an induction motor," in *2012 IEEE International Conference on Power and Energy (PECon)*, 2012, pp. 319–324. doi: 10.1109/PECon.2012.6450230.
- [10] Y. Laamari, K. Chafaa, and B. Athamena, "Particle swarm optimization of an extended Kalman filter for speed and rotor flux estimation of an induction motor drive," *Electrical Engineering*, vol. 97, no. 2, pp. 129–138, 2015, doi: 10.1007/s00202-014-0322-1.
- [11] K. L. Shi, T. F. Chan, Y. K. Wong, and S. L. Ho, "Speed Estimation of an Induction Motor Drive Using an Optimized Extended Kalman Filter," 2002.
- [12] K. Manson, D. Lee, J. Bloemink, and A. Palizban, "Enhanced Fireworks Algorithm To Optimize Extended Kalman Filter Speed Estimation of an Induction Motor Drive System," in *2018 IEEE 9th Annual Information Technology, Electronics and Mobile Communication Conference (IEMCON)*, 2018, pp. 267–273. doi: 10.1109/IEMCON.2018.8614914.
- [13] K. Manson, D. Lee, J. Bloemink, and A. Palizban, "Investigation into Parameter Choice in Use of the Enhanced Fireworks Algorithm to Optimize Noise Covariances used in Extended Kalman Filter Speed Estimation for an Induction Motor

- Drive System,” in 2020 IEEE 29th International Symposium on Industrial Electronics (ISIE), 2020, pp. 61–66. doi: 10.1109/ISIE45063.2020.9152486.
- [14] M. Barut, S. Bogosyan, and M. Gokasan, “Speed-Sensorless Estimation for Induction Motors Using Extended Kalman Filters,” *IEEE Transactions on Industrial Electronics*, vol. 54, no. 1, pp. 272–280, 2007, doi: 10.1109/TIE.2006.885123.
- [15] H. Yu and J. Hu, “Speed and Load Torque Estimation of Induction Motors Based on an Adaptive Extended Kalman Filter,” *Adv Mat Res*, vol. 433–440, pp. 7004–7010, Jun. 2012, doi: 10.4028/www.scientific.net/AMR.433-440.7004.
- [16] B. Song, J. Xu, and L. Xu, “PSO-based Extended Kalman Filtering for Speed Estimation of an Induction Motor,” in 2018 37th Chinese Control Conference (CCC), 2018, pp. 3803–3807. doi: 10.23919/ChiCC.2018.8482581.
- [17] A. Hamid and M. Darfoun, “Artificial Bee Colony Algorithm To Optimize Extended Kalman Filter for Speed Estimation of an Induction Motor Drive System,” Jun. 2024. doi: 10.13140/RG.2.2.21130.07363.
- [18] R. E. Kalman, “A New Approach to Linear Filtering and Prediction Problems,” *Journal of Basic Engineering*, vol. 82, no. 1, pp. 35–45, Mar. 1960, doi: 10.1115/1.3662552.
- [19] R. E. Kalman and R. S. Bucy, “New Results in Linear Filtering and Prediction Theory,” *Journal of Basic Engineering*, vol. 83, no. 1, pp. 95–108, Mar. 1961, doi: 10.1115/1.3658902.
- [20] D. Karaboga and B. Basturk, “Artificial Bee Colony (ABC) Optimization Algorithm for Solving Constrained Optimization Problems,” Jun. 2007, pp. 789–798. doi: 10.1007/978-3-540-72950-1\_77.
- [21] K. Vanchinathan and N. Selvaganesan, “Adaptive fractional order PID controller tuning for brushless DC motor using Artificial Bee Colony algorithm,” *Results in Control and Optimization*, vol. 4, p. 100032, 2021, doi: <https://doi.org/10.1016/j.rico.2021.100032>.
- [22] D. Karaboga, “An Idea Based on Honey Bee Swarm for Numerical Optimization, Technical Report - TR06,” Technical Report, Erciyes University, Jun. 2005.
- [23] T. F. Chan and K. Shi, *Applied intelligent control of induction motor drives*. 2011.
- [24] F. L. Lewis, “Applied optimal control & estimation : digital design & implementation,” 1992. [Online]. Available: <https://api.semanticscholar.org/CorpusID:60695629>
- [25] D. Karaboga and B. Basturk, “On the performance of artificial bee colony (ABC) algorithm,” *Appl Soft Comput*, vol. 8, no. 1, pp. 687–697, Jan. 2008, doi: 10.1016/J.ASOC.2007.05.007.